

Coda wave attenuation for center north of Parecis Basin in the Amazon Craton – Brazil

Lucas Vieira Barros, UnB, Brazil

Marcelo Assumpção, IAG-USP, Brazil

Ronnie Quinteiro, OVISICORI-UNA, Costa Rica

Vinicius Ferreira, UnB, Brazil

Copyright 2009, SBGf - Sociedade Brasileira de Geofísica

This paper was prepared for presentation during the 11th International Congress of the Brazilian Geophysical Society held in Salvador, Brazil, August 24-28, 2009.

Contents of this paper were reviewed by the Technical Committee of the 11th International Congress of the Brazilian Geophysical Society and do not necessarily represent any position of the SBGf, its officers or members. Electronic reproduction or storage of any part of this paper for commercial purposes without the written consent of the Brazilian Geophysical Society is prohibited.

Abstract

Small local earthquakes from two aftershocks sequences in Porto dos Gaúchos, Amazon craton - Brazil were used to estimate the coda wave attenuation in the frequency band of 1 to 20 Hz. The time-domain coda-decay method of a single backscattering model is employed to estimate frequency dependence of quality factor (Q_c) of coda waves. Q_c values have been computed at central frequencies and (band) of 1.5 (1-2), 3.0 (2-4), 6.0 (4-8), 9.0 (6-12), 12 (8-16) and 18 (12-24) Hz in the lapse time ranging from 25 to 60 sec for five different datasets, selected according to the geotectonic environments of the stations locations as well as the ability to sample crustal structures at depths. The well known functional form $Q_c = (Q_0 \pm \sigma) f^{(n \pm \sigma)}$ was determined for all dataset and for the region of Porto dos Gaúchos $Q_c = (117 \pm 19) f^{(1.13 \pm 0.02)}$.

Introduction

Attenuation is a property of the medium and plays an important role in studies of the earth structure and earthquakes sources, from which useful information on the earth structures can be inferred and sources parameters can be determined. Moreover, it is essential to the seismic risk studies, and so has a remarkable application on seismic hazard assessment and consequently to seismic risk mitigation.

The Coda waves from small local earthquakes have been interpreted as superposition of backscattered body waves generated from numerous heterogeneities presented in the ray path distributed randomly but uniformly in the earth lithosphere (Aki, 1969; Aki and Chouet, 1975; Rautian and Khaliturnin, 1978). Coda waves comprise that part of the seismogram composed by different phases that arrive at the station traveling different paths. Therefore the great variety of paths traveled by these waves provide information concerning to the average properties of the medium (attenuation properties) instead of just the characteristics of the particular path (Gupta et al., 1995). The attenuation of the seismic waves in the

lithosphere is highly frequency dependent. This dependence is clearly exponential with the distance and is caused by the combination of two effects: scattering and anelastic attenuation (Havskov et al., 1989) and it is difficult to separate each other, since both have the same mathematical approach (Aki, 1969 and Havskov et al., 1989).

In the present paper, the single scattering model has been used to study the coda Q attenuation in Porto dos Gaúchos Seismic Zone (PGSZ), using small aftershocks earthquakes following the mainshock of 5.2 (MMI VI) on March, 10 1998 and 5.0 m_b (MMI V), on March 23, 2005 (Barros et al. 2009).

Seismicity of the study area

Porto dos Gaúchos Seismic Zone (PGSZ) is located in the center north of Mato Grosso State, in the contact between southern part of Amazonian craton and northern of Phanerozoic Parecis basin (Fig. 1).

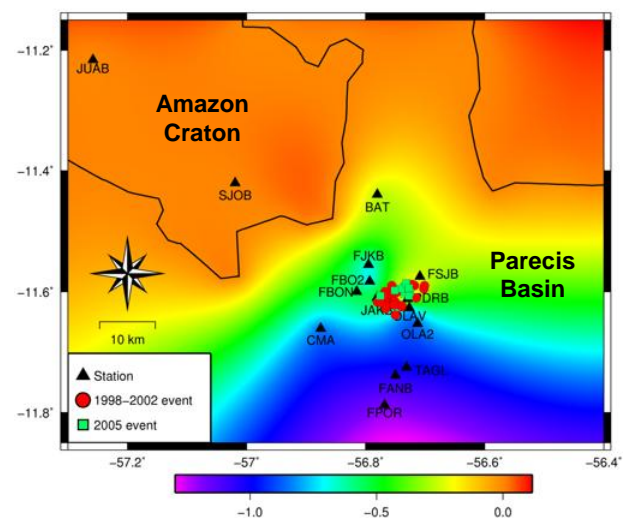


Fig. 1: Topography of the basement in Parecis basin as obtained by Receiver Function technique applied to local events (scale bar in km). Dash line indicates the limit between Amazonian craton and Parecis basin (Barros et al., 2008). Triangles denote seismic stations. Stations OLA2, FBOZ, PDRB, and JAKB belong to 2005 seismic network and station FSJB belongs to both networks. All the rest compose the 1998-2002 network. Stations ending in B are broad-band station (30 sec to 50 Hz) and the rest are short period three-component stations (1 Hz-100 Hz).

In Porto dos Gaúchos a recurrent seismicity has been observed since 1959 (MM Intensity IV-V), two years before the arrival of the first inhabitant in that remote area of the Amazon forest. In the beginning of 1980, with the installation of regional stations in Amazon region, earthquakes with magnitude between 3.5 and 4.4 were detected in subsequent years (in 1981, 1986, 1987, 1988 and 1996), and on March 10, 1998 a 5.2 m_b and MMI VI was detected. A local seismic network was deployed by the Seismological Observatory of the University of Brasília (UnB) just to study the aftershocks activity (Fig. 1). This network, with up to seven three components stations, detected more than 2500 events until December of 2002, when it was disabled, but only 100 of them were located with good accuracy, using a 1D velocity model determined by shallow refraction and a V_p/V_s ratio of 1.70.

On March 23 of 2005 another shock was detected in the same seismogenic area of Porto dos Gaúchos, with magnitude 5.0 (NEIC) and intensity V (MM). One week later five seismic stations were installed by UnB again to monitor the aftershock activity. In three months, this network detected more than 3,500 micro earthquakes, but only 50 events were detected by four or five stations simultaneously. In both case the hypocentral locations were carried out with hypocenter code (Lienert, 1994). For this sequence was used a $V_p/V_s = 1.78$

Coda-Q method

Coda wave for local earthquakes can be explained as backscattered S-waves from lateral heterogeneities distributed uniformly in the lithosphere (Aki, 1969; Aki and Chouet, 1975). The scattering is produced by irregular topography, complex surface geology, elastic property of the rocks, faults and cracks, which are more near the surface and less in deep region (Kumar et al., 2005). This implies that coda wave amplitude decay as a function of lapse time (time measured from the origin time) for different earthquake in a given area parallel each other, independently of the source and receiver locations (Biswas and Aki, 1984). The decrease of coda wave amplitude with lapse time, according to Aki (1969), at a particular frequency, is only due to energy attenuation and geometrical spreading but independent of earthquake source, path propagation and site amplification. The attenuation of seismic waves is the sum of intrinsic and scattering attenuation, where in the first case the energy is converted in heat through anelastic absorption and in the second case it is redistributed through refraction, reflection and diffraction at random discontinuities present in homogeneous medium (Kumar et al., 2005).

After the advent of coda wave theory by Aki, (1969) and Sato (1977), many studies (e.g. Aki and Chouet, 1975; Rautian and Khalturin, 1978 Kumar et al., 2005) have shown that the coda Q factor increases with frequency through the relation

$$Q(f) = Q_0 \left(\frac{f}{f_0} \right)^\eta \quad (1)$$

Where Q_0 is the quality factor in the reference frequency, f_0 , usually 1 Hz and η is the frequency parameter, which is close to the unity and varies from region to region according to the heterogeneities of the medium (Aki, 1981; Kumar et al., 2005). Q_0 and the frequency parameter are variable according to the seismicity, tectonic and geological features of each region.

Assuming a single scattering from randomly distributed heterogeneities, Aki and Chouet (1975) have shown that the coda wave amplitude at frequency, f , and elapsed time, t , from the origin can be expressed as:

$$A(f, t) = S(f) t^{-\nu} e^{-\pi f t / Q(f)} \quad (2)$$

Where $S(f)$ is the source function at a frequency f , ν is the geometrical spreading parameter and $Q(f)$ the coda wave attenuation quality factor (Q_c), representing the attenuation of the medium. $S(f)$ is considered a constant (as it is independent of time and radiation pattern) and, therefore, not a function of those factors influencing energy loss in the medium. The parameter ν can assume the values 1.0 (for body wave scattering), 0.5 (for surface wave scattering) and 0.75 (for diffusive waves). As coda waves are S to S backscattered shear waves (Aki, 1981), the spreading parameter $\nu = 1$ is used in this study. The equation 2 is valid only if the coda start window begun at least after two times the S wave propagation time $2(T_s - T_0)$ to avoid in the coda window the data of direct S-wave and to validate the assumption used in the model that receiver and source are coincident (Rautian and Khalturin, 1978).

Taking the natural logarithm of the equation 2 we obtain

$$\ln A(f, t) + \nu \ln(t) = \ln(S(f)) - \pi f t / Q(f) \\ \ln[A(f, t)t] = K - b t \quad (3)$$

The above equation represents a straight line where $b = \pi f / Q_c$ and $K = \ln(S(f))$.

Hence, Q_c can be obtained by linear regression from the slope of the $\ln[A(f, t) * t]$ versus t curve on a constant frequency. Then, in order to determine Q_c the seismogram is initially narrow-band-pass filtered using the routine in Havskov and Ottomöller (2008) at different central frequencies and for each band Q_c is determined, as it will be seen in the next section.

Data selection and analysis

The choice of used data for analysis was preceded by a careful selection, where it was observed events magnitudes, stations location, events epicentral distance, tectonic environment of the stations location, data sampling rate, events depths etc. The events magnitudes range from 1.2 to 3.4 m_D , and the epicentral distances ranging between 1.0 km (JAKB and PDRB stations) to 72 km (JUAB station). The two seismic sequences (1998-2002 and 2005) were monitored by two different seismography networks. In the first case, the stations were installed further from the source with stations installed in the Amazon craton (JUAB and SJOB) an in the Parecis basin (BAT, FJKB, FSJB, CMA, FANB, TAGL, FPOR). See Fig. 1 for stations location. JUAB station was

the first to be installed, thus the events occurring between March 1998 to May 1999 were detected only by the JUAB station and two analog stations, not shown in Fig. 1.

In both networks were used broadband (Guralp CMG-40T, 30 s to 50 Hz) and short period three-component (3C) seismic sensors (S3000EQ, 1.0 Hz to 100 Hz). The dataloggers used were Quanterra (QDAS-4120) and Nanometrics (ORION), both with wide dynamic range (> 130 dB). The sampling frequency was 100 Hz; however, the instrument Quanterra recorded many events at a rate of 20 sps (in continuous recording mode). Events with this sample rate (20 sps) were rejected by the high cutoff frequency filter criteria. The three-component broadband stations have identification code ending in B. All the rest are short period 3C stations.

Data was grouped by different geotectonic environments as well as the ability to sample structures at depths, depending on the events focal depths and the thickness of the sedimentary package in the station location, which is shown to be a determining factor in the frequency response of the Coda Q waves. In this sense, the events could be divided into five different groups: group A – 19 events from the 2005 seismic sequence, all recorded by stations located in the Parecis basin (FBO2, JAKB, FSJB, PDRB and OLA2); group B: 28 events from the 1998-2002 seismic sequence, recorded by stations located in Parecis basin (BAT, FJKB, FBON, FSJB, OLAV, TAGL, CMA and FPOR); group C - all the events of both groups A and B (47 events), registered by both set of stations of 1998-2002 and 2005 networks; group D: 39 events from 1998-2002 sequence recorded by stations located in the Amazon craton (SJOB and JUAB stations) and; Group E: all events recorded in the basin and the Craton (groups C and D = 96 events) registered by both networks.

The sequence of events from the 1998 to 2002 occurred at shallow depths, between the surface and just over 6.0 km, and the vast majority, around 70%, had foci between 3.0 km and 6.0 km. But the events sequence of 2005 was more superficial. The deepest reached only 3.0 km deep. Therefore, the events of groups A and B should show different volumes of Parecis basin.

Aiming to test the sensitivity of Coda waves to the thickness of the basin sedimentary package the group C events were divided into two subgroups: subgroup C1, composed by events recorded by stations located in the northern part of the abrupt transition on the depth basin, six stations (BAT, FJKB, FSJB, FBO2, FBON and PDRB), and subgroup C2, events recorded by stations located to the southern of the transition, six stations (CMA, JAKB, OLAV, OLA2, TAGL and FPOR). See Fig. 1 for station locations.

The events were selected afterwards to test several values of the signal noise ratio (S/N) and the correlation coefficient (CO). It was found that S/N = 2 and CO = 0.45 represent a good compromise between to rejecting too much data and getting a reasonable dispersion in average Q for each group of events. For the beginning of

Coda window the same value $2(T_s - T_0)$ is always adopted. The length of the coda window (lapse time) ranged between 25 to 60 seconds, in steps of 5 seconds.

Six different central frequencies (1.5, 3.0, 6.0, 9.0, 12.0 and 18.0) are used in the band of (1-2, 2-4, 4-8, 6-12, 8-16 and 12-24 Hz), respectively. Fig. 2 shows two examples of raw data seismograms (on the top of both figures) and band pass filtered seismograms in the six central-frequencies and band-pass mentioned above. The first signal was registered by the broadband 3C station JUAB distant 70 km from the source. The second one was recorded by 3C short period station OLA2, located 4 km from the source. Both signals were sampled at a rate of 100 sps (sample per second).

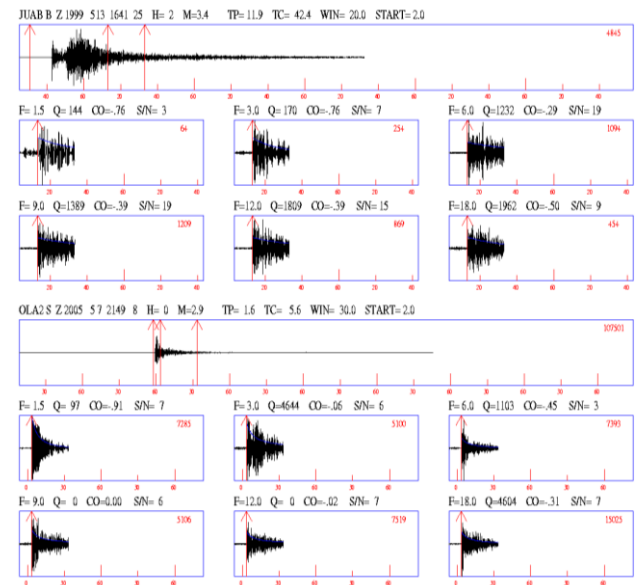


Fig. 2: Examples of unfiltered and band pass-filtered traces for two events registered at different distances from the source and at different depths. The first registered by distant cratonian station JUAB (70 km from the source) during the 1998-2002 sequence and the second registered by close basin station OLA2 (4 km) during 2005 seismic sequence. In each figure, the top trace is the original unfiltered signal where the 3 vertical lines indicate (from the left) origin time (T_0), start and end of the coda window. On top of first trace is shown the station code and event identification. The abbreviations are: H=depth (km); M=coda magnitude; TP=P onset time; TC= start of coda window measured (in sec) from the origin; win=window length start=start of coda window in terms of S travel time, always = $2(T_s - T_0)$; f=frequency in Hz; CO=correlation coefficient; and S/N= signal-to-noise ratio of the last 5 sec of the coda signal used by the correspondent first 10 sec of noise window. The fit envelope of each filtered segment is shown as a decay curve for six central frequencies as described on the text.

The six envelopes of the coda waves, one for each central frequency, shown on the left corner of each envelope figure (see Fig. 2) were determined for two different lapse times. Upper trace, 20 seconds and lower trace 30 seconds. The shape of each envelope depends on basically of two key parameters: the signal to noise ratio (S/N) and the correlation coefficient (CO).

Results

The estimates of quality factor have been determined for five different datasets, each one representing a particular configuration of stations-location in relation to the seismic source. Estimates of Q_c to datasets A and B aim to evaluate the effects of the seismic network aperture in the coda waves attenuation characteristics; Estimates on dataset C and D aim to determine coda Q factor for two different areas: Parecis basin (dataset C) and Amazon craton (dataset D). The average Q_c values for the region was obtained using the dataset E (dataset C plus dataset D). The results for these areas are: Group A data, $Q_c = (89 \pm 9)f^{(1.16 \pm 0.12)}$; Group B data, $Q_c = (120 \pm 12)f^{(1.08 \pm 0.09)}$; Group C data, $Q_c = (111 \pm 12)f^{(1.10 \pm 0.08)}$; Group D data, $Q_c = (175 \pm 46)f^{(1.01 \pm 0.04)}$ and group E data $Q_c = (117 \pm 19)f^{(1.13 \pm 0.02)}$.

To evaluate and compare the differences in the behavior of the coda waves for different lapse times in terms of the quality factor in the reference frequency (Q_0) and frequency parameter (η) it is presented plots for all data groups in Fig. 3: (a) Quality factor at a frequency of 1 Hz (Q_0) versus lapse time and (b) frequency parameter (η) versus lapse time.

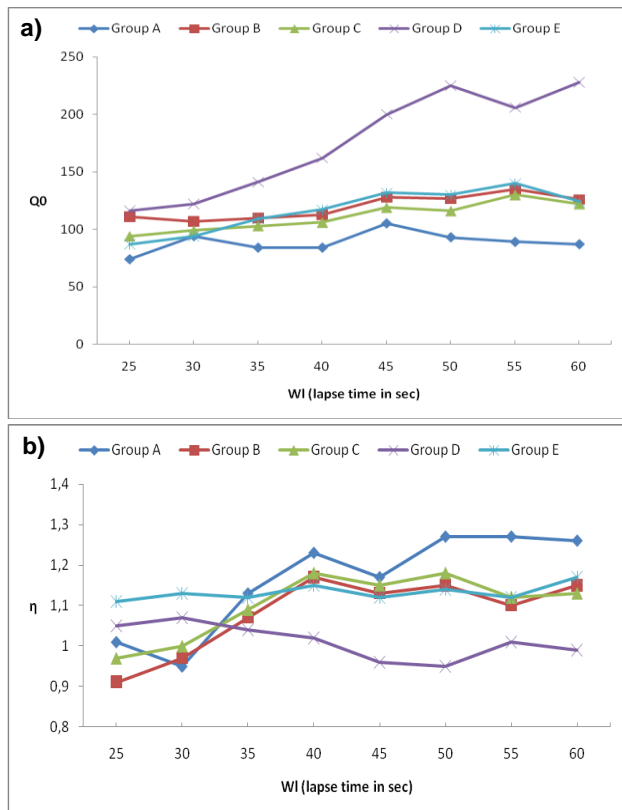


Fig. 3: Plots of quality factors at a frequency of 1 Hz (Q_0) and frequency parameter (η) with lapse time for all data groups, (a) Q_0 with lapse time for all data groups and (b) frequency parameter (η) with lapse time for all datagroups.

The results for subgroups C1 and C2 are, respectively: $Q_c = (121 \pm 17)f^{(1.09 \pm 0.08)}$ (for northern) and $Q_c = (84 \pm 15)f^{(1.18 \pm 0.14)}$ (for southern). In Fig. 4 are presented the results of the quality factor (Q_c), quality factor at a frequency of 1 Hz (Q_0) and frequency parameter (η) for the region (group E data). (a) Quality factor (Q_c) versus lapse time for six central frequencies analyzed, (b) Quality factor at a frequency of 1 Hz (Q_0) and frequency parameter (η) versus lapse time.

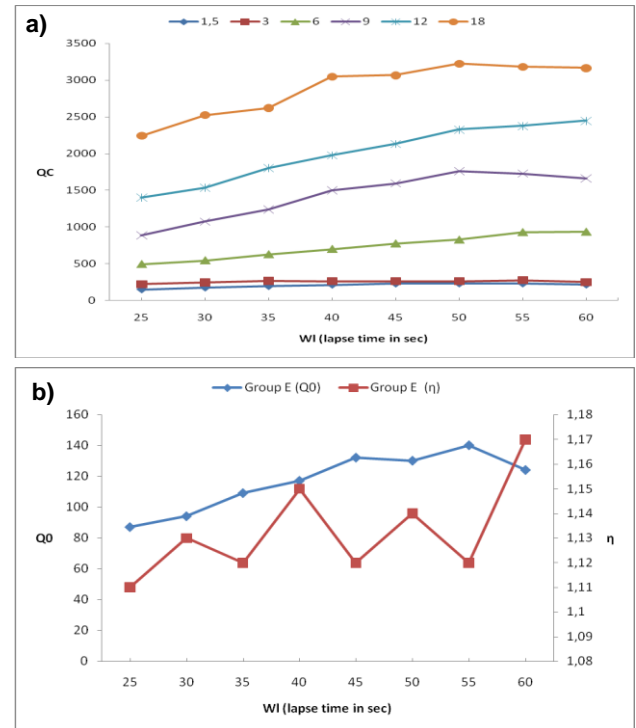


Fig.4: Plot of average Q_c , Q_0 and η against lapse time for all stations and data groups (C and D) together (group E data). (a) Average Q_c with lapse time at different frequencies and (b) average Q_0 and frequency parameter η against lapse time.

7. Discussion

The results of the average quality factor (Q_c) for coda waves, estimated by linear regression for the five data groups in six frequency bands are slightly different, both with respect to the values of coda Q factor at a frequency of 1 Hz (Q_0), and values of the frequency parameter (η). This can be explained by the fact that each data group samples different volumes of geological data, both due to the positions of stations in relation to the seismic source (distance) as well due to their locations in each geotectonic environment. Thus, the lateral heterogeneities present in the seismic ray's paths are quite different, and affect, therefore, in different forms the Coda wave energy.

A relevant fact to these results concerns the two geotectonic environments sampled by Coda waves:

Fanerozoic sediments of Parecis basin, where is located the seismogenic fault and pre-Cambrian basement of Amazon craton. Moreover, the thickness of the sedimentary basin varies greatly from north to south (Fig. 1) and, depending on the position of the seismic station, the Coda waves travel more by sediment or more by the basement; two contrasting environments in terms of rock density, body wave propagation velocity and presence of heterogeneities. All these factors affect differently the amplitudes of Coda waves with lapse time. Stations most distant from the source sample deeper structures, and in this case sample the crystalline basement of Amazon craton, where the rocks are denser, homogeneous and with higher speed of body waves. This generally equates to an increase in coda quality factor Q_c (inverse of the seismic attenuation quality factor) due to mainly a reduction in heterogeneities. The results gotten for Groups A and B data, clearly show this. Group A data – stations are close to the source and events foci shallow, $Q_c = (89 \pm 9)f^{(1.16 \pm 0.12)}$; Group B data – stations are more distant and events foci even deeper, $Q_c = (120 \pm 12)f^{(1.08 \pm 0.09)}$. Therefore different structures should be represented by these differences observed in coda wave's frequency response, either because the distances of the recording stations but also due to depths of seismic sources. For Group A, the events are more shallow and close implying in lower Q_0 (89) and higher η (1.16), and for Group B more distant and deeper Q_0 is higher (120) and η is lower (1.08). Then, the reduction in Q_0 can be explained by the decrease in heterogeneities with depth, and the increase in η should be understood as the presence of lower wavelengths discontinuities present in the sediments and detected only by high frequency coda waves. The results for the basin area. $Q_c = 111f^{(1.10)}$, for the craton, $Q_c = 175f^{1.01}$, and for the region, $Q_c = 117f^{(1.13)}$ can be explained as well.

In Figs 3(a) and 3(b) it is presented the quality factor at a frequency at 1 Hz (Q_0) and frequency parameter (η) for all data groups against lapse times. The curves for group A and group D occupy extremes in alternative positions in the graphics. These results emphasize the conclusion that the behavior of coda waves reflects the type of geological environment in the subsurface. The greatest value of Q_0 (175) in the Craton and the lower Q_0 (89) to the basin should be associated with bigger homogeneity of the rocks on basement craton, while the higher value of η for the basin should be related to the presence of many and small discontinuities (heterogeneities) common to a sedimentary environment. Moreover, the volume of rock sampled by the Group A data is the most representative of the seismogenic fault, where the basement rocks underlying the sediments must be broken and fractured, implying in a lower Q_0 .

The effects of the sediments layer thickness in the coda waves attenuation is very clear if we compare the results of coda Q factor, coda Q factor at a frequency of 1 Hz and frequency parameter gotten to the subgroups data C1 (Northern stations) and C2 (Southern stations). For northern part of Parecis basin, $Q_c = (121 \pm 17)f^{(1.09 \pm 0.08)}$

and for the southern, $Q_c = (84 \pm 15)f^{(1.18 \pm 0.14)}$. This shows that the energy of coda waves are attenuated more strongly in the sediments (southern part where sediment layer is thicker) than in the basement (lower Q_0 in the sediments, $Q_0=84$) and they are more sensitive to high frequencies (higher frequency parameter, $\eta=1.18$). Thus, the coda waves can be used to infer geological structures in subsurface, as the coda quality factor average values and frequency parameter demonstrated to be highly dependent on the sedimentary layer thickness.

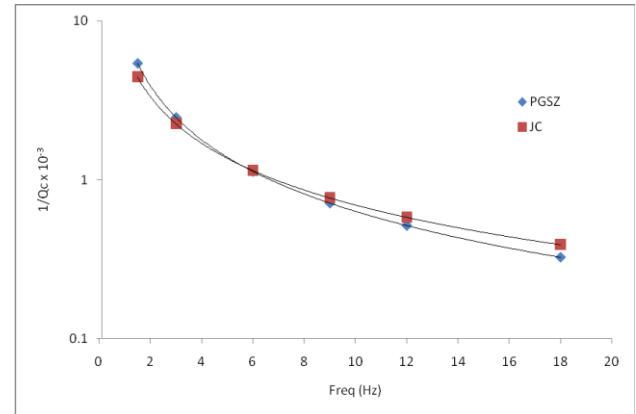


Fig. 5: Comparatives results of $1/Q_c$ versus frequency to João Câmara region (JC) and Porto dos Gaúchos seismic zone (PGSZ).

Fig. 4a shows the dependency of Q_c on frequency. The increase in values with the increase in frequency indicates the frequency dependence nature of Q estimates in region. Similar results were gotten by Dias and Souza (2004) to João Câmara region, Northern of Brazil (Fig. 5).

8. Conclusion

The observed differences in the values of $Q(f)$ are associated with the tectonic-sedimentary environment sampled by each data group. In the group C data, are found two distinct geological media: sediment of the Parecis basin and crystalline basement of the Amazonian craton underlain the Parecis basin sediment layer; for Group D, mainly the crystalline basement of the Amazon Craton and; for Group E, an average of the average values of the coda factor (Q_c) for these two areas.

The sensitivity of Coda waves to the thickness layer of the basin sedimentary is unquestionable. The $Q(f)$ estimated values for the two cases clearly show that: In Group C1 (northern basin), six stations located in locals where the sediment package is thinner (100 m to 300 m) $Q_c = (121 \pm 17)f^{(1.09 \pm 0.08)}$; to group C2 (southern basin), six stations located in locals where the sedimentary package is thicker (300m-1400m), $Q_c = (84 \pm 15)f^{(1.18 \pm 0.14)}$. It should be mentioned that the same set of event was used, both registered by six

stations in such way that the average lapse time of Coda waves for the two cases is more or less the same for the eight time windows. This ensures that the differences in the values of $Q(f)$ must be related to the scattering numbers (heterogeneities) present in both areas.

So, it is possible to conclude that the application of coda Q method on local earthquakes, besides giving information on seismic wave energy attenuation and earthquake source parameters, can be used to infer useful information on earth structures.

9. References

- Aki, K., 1969.** Analysis of seismic coda of local earthquakes as scattered waves, *J. Geophys. Res.* 74, 615-631.
- Aki, K., 1981.** Source of scattering effects on the spectra of small local earthquakes. *Bull. Seismol. Soc. Am.* 71, 1687-1700.
- Aki, K. and Chouet, B., 1975.** Origin of the coda waves: source, attenuation and scattering effects, *J. Geophys. Res.* 80, 3322-3342.
- Barros, L.V., Assumpção, M., Quintero, R. and Caixeta, D. 2009.** Porto dos Gaúchos Seismic Zone in the Amazon Craton – Brasil. *Tectonophysics* doi:10.1016/j.tecto.2009.01.006
- Barros, L.V., Assumpção, M., Quintero, R. and Paz, R.N., 2008.** Basement Topography using P-to-s conversions from local earthquakes in the seismogenic area of Porto do Gaúchos, Parecis basin, Northern Brazil. Joint assembly AGU. Florida-USA
- Biswas, N.N., Aki, K., 1984.** Characteristics of coda waves: Central and Southcentral Alaska. *Bull. Seism. Soc. Am.*, Vol. 74, No. 2, 493-507.
- Dias, A.P., Souza, J.L., 2004.** Estimates of coda Q attenuation in João Câmara area (Northeastern Brazil). *Journal of Seismology* 00 1-12.
- Gupta, S.C., Singh, V.N. and Kumar, A.I., 1995.** Attenuation of coda waves in the Garhwal Himalaya, India. *Physics of the earth and Planetary Interiors*, 87, 247-253
- Havskov, J. and Ottemoller, L. 2008.** SEISAN: The Earthquake Analysis Software for Windows, Solares, Linux and Macosx, Version 8.2.1. Institute of Solid Earth Science, University of Bergen, Norway.
- Havskov, J., Malone, S., McClurg, D. and Crosson, R. 1989.** Coda Q for the State of Washington. *Bull. Seismol. Soc. Am.* Vol 79, No. 4, 1024-1038.
- Kumar, N., Parvez, I.A. and Virk, H.S. 2005.** Estimation of coda wave attenuation for NW Himalayan region using local earthquakes. *Physics of the Earth Planetary Interiors* 151, 243-258.
- Lienert, B.R., 1994.** Hypocenter 3.2: A computer Program for locating earthquakes locally, regionally and globally. Hawaii Institute of Geophysics and Planetology
- Rautian, T.G. and Khalturin, V.I. 1978.** The use of the coda for determination of the earthquake spectrum, *Bull. Seism. Soc. Am.* 68, 923-948.
- Sato, H., 1977.** Energy propagation including scattering effects, single isotropic scattering approximation, *J. Phys. Earth* 25, 27-41.